# HYDRODYNAMICS OF BEATING CILIA

ANTOINE DAUPTAIN, JULIEN FAVIER AND ALESSANDRO BOTTARO
DICAT, Università di Genova, via Montallegro 1, 16145 Genova, Italy

**Abstract** A numerical approach is developed to study the effect on a fluid of the regular oscillations of an array of flexible cilia which hinge around points on a wall. The specific application studied concerns the ctenophore *Pleurobrachia pileus*, a small marine invertebrate of quasi-spherical shape and diameter of the order of the centimeter which swims in water thanks to the rhythmic beating of eight rows of hair-like cilia aligned along its body. Only one row of cilia is studied here, and the paper is limited to two-dimensional flow cases. The technique presented is however general enough to allow its application to a variety of fluid-structure interaction problems. Results show that the expended power increases with the increase of the beating frequency, in qualitative agreement with experiments.

## 1. Introduction

### General scope

Cilia and flagella are little-noticed but pervasive features of animals and plants, accomplishing - through their movement or simply through their presence - a large variety of tasks [1]. Motile cilia are whip-like appendages extending from the surface of many types of cells, and designed to move either the cell itself or the fluid around it. Their behavior is a consequence of their complex internal structure, which is essentially the same in both eukaryotic flagella and cilia, and is based on the interaction of a set of microtubules. These can bend under the action of dynein arms, powered by ATP, thus generating typical oscillations. Progress in the computational modelling of the internal axoneme of a flagellum has been recently reviewed by Fauci & Dillon [2]. From the "external" point of view, the major differences between motile cilia and flagella can be seen *(i)* in their length, *(ii)* in the fact that cilia appear in densily packed arrays, whereas flagella act mostly individually or in couples, and *(iii)* in the characteristics of their beating which determines the direction of the induced thrust.

Though this paper will be devoted to a very specific kind of ciliary motion, it is not useless to briefly outline a few of the functions played by such organelles, to provide an idea of their usefulness and broad range of applications:

- a single flagellum is used by sperm cells to move forward;
- in all female mammals, the beating of cilia in the Fallopian tubes moves the ovum from the ovary to the uterus;
- about 80% of the epithelial cells in the human trachea are ciliated. Cilia sweep mucus and trapped particles into the throat where they are usually swallowed and expelled;
- the cochlea in the inner ear is lined with cilia, which oscillate after sensing vibrations transferred from the middle ear thus triggering the generation of nerve impulses, conveyed to the brain as bursts of acoustic information;
- the asymmetric motion of embryonic fluid produced by beating cilia affects the expression of genes located on the left hand side of the embryo of many vertebrates. The same genes remain inactive on the right hand side of the body, thus apparently determining inner organ placement and the left-right asymmetry in the body axis [3];
- ciliary defects can lead to several human diseases [4].

The interaction between cilia and flagella with their environment has attracted in the last half century the interest of physicists and engineers, motivated also by the possible use of ciliated actuators as micro-mixers, for flow control in tiny biosensors, or as micropumps for drug-delivery systems.

The study of the hydrodynamics of a beating flagellum was initiated in 1951 by G.I. Taylor [5] who analyzed the locomotion induced on a body by a tail beating in a regular manner, and found an approximate relation linking the velocity of the organism to the propagation speed of the tail wave. Other studies followed in which many cilia, covering flat or curved surfaces and oscillating synchronously, were considered and for which local models of the hydrodynamic interactions between cilia and the surrounding fluid were needed. These research activities were initiated with the observation that organisms appear to benefit from adjusting the phase relationship of the beat patterns of neighboring cilia, and that metachronal waves are the rule in the oscillations of cilia and flagella. The early activity is comprehensively reviewed by Brennen & Winet [6], and is mostly focussed on isolating and understanding aspects of the self-propelling behavior. To simplify things, inertial effects were neglected, because of the small dimensions and low velocities at play. The more or less densely packed arrays of cilia were treated by local interaction models which, despite the approximations made, were quite successful at reproducing global features of the motion. They can be grouped into two categories: the *envelope* model [5, 7, 8, 9, 10, 11] and the *sublayer* model [9, 10, 12, 13, 14]. In the envelope model the cilia are assumed to be closely packed together so that the fluid effectively sees a waving material surface enveloping the top of the layer. The principal limitations of this approach lie in the small amplitude approximation for the oscillations of the material surface and in the impermeability and no-slip condition imposed at the envelope sheet. The sublayer approach is not limited to small amplitudes and models the distribution of Stokes flow force singularities along each cilium with an equivalent body force. The key assumption here is in how the interaction among individual cilia is modelled: in the formulation by Blake [9] such an interaction force is steady, whereas Keller, Wu and Brennen [12] improved the model by including unsteadiness. Both the envelope and the sublayer approach yield results in qualitative agreement with observations in their respective ranges of applicability. Clearly the details of the hydrodynamics within the cilia array and the effect of possibly non-negligible inertial terms posed problems which, until recently, were overwhelming.

In more recent times, advances in experimental techniques have rendered the problem amenable to laboratory investigation and some papers appeared which questioned the hydrodynamic results of the proposed models [15, 16]. Progress in computational fluid dynamics and in the available hardware make the problem tractable also by a numerical approach.

**Configuration studied**

To fix things we have considered a very specific case, the locomotion characteristics of the ctenophore *Pleurobrachia pileus* (commonly known as the "sea gooseberry") which, as we will see below, is outside the range of approximation of former models. In such a small organism (*cf.* figure 1) the thickness of the layer of cilia is much smaller than the body dimension, so that it is appropriate to consider a flat layer of cilia exhibiting planar beat patterns. Propulsion is produced by the oscillations, at a particular frequency, of eight rows of comb plates, disposed around the body and aligned with it, each one of which is composed by hundred thousands or more cilia. The beating pattern exhibits an antiplectic metachronism, *i.e.* each individual cilium (or comb) presents a definite phase relationship with its neighbours, and the wave propagates in a direction opposite to the effective stroke. We will study the influence of beating parameters on the power

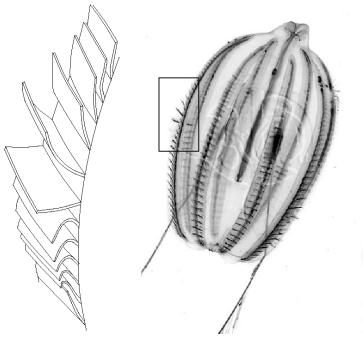

*Figure 1.* Propulsive row of comb plates on a *Pleurobrachia*.

output of the mechanism. Different beating patterns will be tested, covering an appropriate range of frequencies and wavelengths.

Figure 2a shows the positions occupied by a cilium within one time period of the antiplectic wave; during the effective stroke (towards the left) the cilium is straight, while in the recovery phase it is bent so that a significant portion of it moves tangentially to the induced stream, rather than normally. Considering an array of cilia, to model the *Pleurobrachia*'s comb plates, when metachronal strokes are brought towards the left, a right-propagating wave is produced and the body is propelled to the right (*cf.* Figure 2b). The aim of this paper is to focus on this propulsive mechanism, by looking at the action of a comb row on the surrounding fluid.

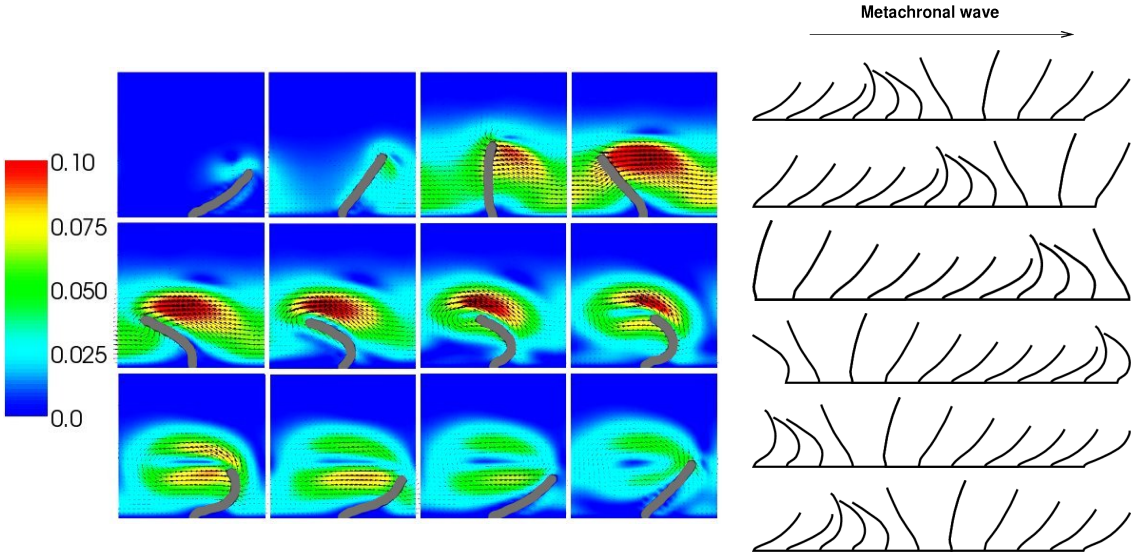


(a) Motion of a single cilium starting from rest. (b) One antiplectic period.

*Figure 2*. Antiplectic beat pattern of the cilia of the *Pleurobrachia*. (a) Successive images, equally spaced in time, must be seen as in a comic strip. The color scale represents the amplitude of the velocity vectors. (b) Time increases from top to bottom; the organism is propelled towards the right, in the same direction as the metachronal wave.

## 2. Numerical procedure

Cilia position and velocity are digitized from experimental data and imposed by using an immersed boundary method (IBM) [17]. The Reynolds number, based on tip speed of the cilium, its length and the kinematic viscosity of water, ranges from 50 to 200; since the Stokes approximation is not tenable, two Navier-Stokes codes are tested to solve the incompressible laminar flow problem: NTMIX [18] (8th order in space, 3rd order in time with an explicit scheme, variables are not staggered in the grid), and BRUTUS (2nd order in space and time with a predictor-corrector scheme, staggered variables). The numerical resolution is performed by decomposing the main problem into three subproblems (extraction of position and velocity of cilia, IBM, fluid problem) that are controlled by a coupler, PALM [19], to ensure a straightforward development towards more general applications for fluid-structure interaction problems.

### Validation

To validate the numerical tool two configurations are considered: in the first test case a two-dimensional rigid plate of length $L$ hinges on a point in the lower wall and beats periodically; the domain of integration of the equations is square ($2L \times 2L$); lower and upper boundaries are no-slip walls, left and right boundaries are periodic. The lower extremity of the plate is centered in the lower wall, and the angle formed by the plate with the vertical axis is $\alpha(t) = \frac{\pi}{4}\cos(2\pi f t)$, with $f$ the beating frequency (*cf.* figure 3a). The numerical discretization employs a regular $32 \times 32$

cartesian grid. The second test case considers the motion of a single deformable cilium; such a movement replicates the measurements by Barlow *et al.* [16] (see figure 3b). The computational domain in this case is rectangular ($2L \times 4L$) and the grid is composed by $32 \times 64$ regularly distributed points. The cilium is decomposed into 40 identical segments, and its motion is described by the angular deviation between one segment and its immediate neighbors. The angular position and velocity of each segment is obtained from a look-up table and a simple linear interpolation in time is performed to obtain these data at the discrete time levels of the computations. Within one beat cycle we can perform several thousand time steps and hence we need the same number of intermediate cilium's positions, whereas Barlow *et al.* [16] provide data for 12 intermediate positions. For the characteristic case of $f = 20$ Hz and $L = 1$ mm, the maximal velocity attained at the tip is $\pi^2 L f/2 = 98.7$ mm/s. Thus, the Reynolds number in water is of order one hundred.

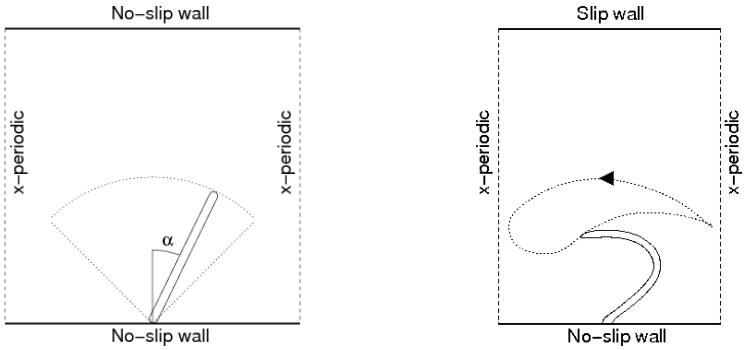


(a) Beating rigid plate. (b) Beating flexible cilium.

*Figure 3.* Test cases considered. In case (b), the arrow shows the trajectory of the tip of the cilium.

**Immersed Boundary methods**

The accuracy of imposing a prescribed time-dependent velocity field within the flow has been tested for a few different implementations of the IBM, along the lines of Fadlun *et al.* [20]. To match the cilium velocity distribution $\mathbf{V}$ to that on the boundary $S$ corresponding to the cilium position, a volume force field $\mathbf{f}$ is introduced in the computational domain. The incompressible Navier-Stokes equations are then:

$$\frac{\partial \mathbf{u}}{\partial t} + (\mathbf{u} \cdot \nabla)\mathbf{u} = -\nabla p + \nu \nabla^2 \mathbf{u} + \mathbf{f}\,;\; \nabla \cdot \mathbf{u} = 0. \tag{1}$$

Two strategies are examined to specify numerically the proper volume force field:

- According to a technique which we call the *feedback forcing technique*, the volume force $\mathbf{f}$, for a solid boundary located at $\mathbf{x}_s = (x_s, y_s)$ at time $t$ and moving at speed $\mathbf{V}$, is defined as:

$$\mathbf{f}(\mathbf{x}_s, t) = \alpha_f \int_0^t \left[\mathbf{u}(\mathbf{x}_s, t) - \mathbf{V}(\mathbf{x}_s, t)\right] dt' + \beta_f \left[\mathbf{u}(\mathbf{x}_s, t) - \mathbf{V}(\mathbf{x}_s, t)\right]. \tag{2}$$

  In this expression $\alpha_f$ and $\beta_f$ are negative constants, heuristically determined so that a measure of the difference $\mathbf{u}(\mathbf{x}_s, t) - \mathbf{V}(\mathbf{x}_s, t)$ is minimized. This formulation displays a damped oscillator's behavior, with $\alpha_f$ proportional to the frequency of the oscillations and with $\beta_f$ a damping factor. This method is implemented in the numerical solver NTMIX.

- A second approach, known as the *direct forcing method*, is based on the discrete expression of the Navier-Stokes equations. Indicating with $l$ the discrete time level, and with $\mathbf{RHS}$ the vector containing the viscous, convective and pressure terms, one obtains:

$$\mathbf{f}^{l+1}(\mathbf{x}, t) = \frac{\mathbf{V}^{l+1} - \mathbf{u}^l}{\Delta t} - \mathbf{RHS}^l. \tag{3}$$

  The advantage of this method is that no tunable constants are required; the implicit algorithm proposed by Fadlun *et al.* [20] is implemented in BRUTUS.

A second crucial step in the IBM is the interpolation strategy. This is even more delicate in the present setting, because of the rapidly moving boundary, and the small dimensions of the moving bodies. Indeed, the position of each cilium is specified in the continuum and in the feedback forcing technique the volume force $\mathbf{f}(\mathbf{x}_s, t)$ must be distributed among the grid points surrounding the bodies in motion. In the direct forcing approach, it is a measure of the discrete target velocity $\mathbf{V}^{l+1}$ that must be applied to the appropriate grid points. Two kinds of techniques are used in this paper, for each of the two volume forcing approaches tested: one is called the "distribution strategy" and the second is the "linear interpolation strategy".

We start by observing that each cilium is made up by $M$ points, and moves in a computational domain containing about $N^2$ cells, with $M > N$ (for example $M$=40 and $N$=16). In the "distribution strategy", inspired by Peskin [21], for each of the $M$ points within a cilium $\mathbf{x}_s$, the closest cells $\mathbf{X}_{i,j}$ in the grid are searched for. The indices $i$ and $j$ indicate, respectively, the discretization nodes along the wall-parallel direction, $x$, and the wall-normal direction, $y$; the corresponding velocity components are called $u$ and $v$. The properties of the cilium are spread among the 24 grid points neighboring $\mathbf{X}_{i,j}$ by multiplying either the discrete forcing function or the target velocity by a filter function $h(i, j; \mathbf{x}_s)$ (*cf.* figure 4a). When a grid point $\mathbf{X}_{i,j}$ is influenced by more than one $\mathbf{x}_s$ an averaging procedure is performed. The chosen filter function is:

$$h(i,j;\mathbf{x}_s) = \frac{1-\tanh\left(\frac{r-1}{0.5}\right)}{2}\,;\; r = \sqrt{\left(\frac{x_s - X_{i,j}}{\Delta x}\right)^2 + \left(\frac{y_s - Y_{i,j}}{\Delta y}\right)^2}\,. \tag{4}$$

In the "linear interpolation strategy", when two successive points within the discretized cilium cross a computational grid line, for example when the cilium intersects the horizontal line $j = 4$ (see figure 4b), a linear interpolation is applied to the two horizontal cells to the left and to the right of the intersection point. A similar procedure is carried out when the cilium crosses a vertical grid line. In the figure, the grid point labelled with $i = 3, j = 4$ is hence evaluated twice (with an interpolation along the horizontal axis $j = 4$, and with another interpolation along the vertical axis $i = 3$); the two components of the velocity in that grid point are finally obtained through simple averaging.

In the feedback forcing approach, the volume force $\mathbf{f}(\mathbf{x}_s, t)$ is applied to all the points in the discretization stencil; all other nodes have no source term applied to them. For the direct forcing technique, to obtain the velocity field $\mathbf{u}_{i,j}^{l+1}$ we initialize with $\mathbf{u}_{i,j}^{l}$, and correct the velocity components in the stencil around the cilium on the basis of $\mathbf{V}(\mathbf{x}_s, t)$ at time step $l + 1$.

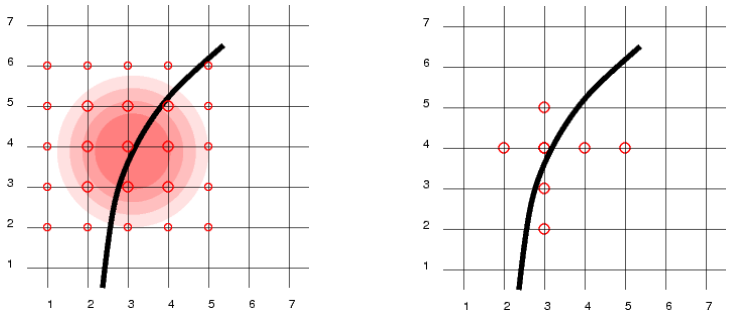


(a) Distribution strategy. (b) Linear interpolation strategy.

*Figure 4*. Interpolation strategies; all the grid points in the discretization stencil are represented with open circles.

An extensive study has been conducted to assess the best technique to treat this moving boundary problem. It appears that the feedback forcing technique is very interesting with NTMIX at very low speed (*e.g.* CFL number around 0.001, $\alpha_f = 0$ and $\beta_f = -1 \times 10^5$). It gives a very good precision when coupled with the distribution strategy, even though the numerical cost is high. Using a non-zero value of $\alpha_f$ leads to unstable simulations, because of the high frequency displacement of

the inner moving boundary. The direct imposition technique and linear interpolation strategy implemented in BRUTUS allow to run simulations with larger CFL numbers (of order 0.5), thus much faster and with an acceptable accuracy.

The large variations in the amplitude of the velocity and in the direction of the different segments which compose a cilium - and the way the exact movement of the body is discretized in the available grid - can be represented in several manners; we have chosen to display them plotting the $u$-velocity component against the $v$-component of different points on the cilium in the course of time. Such a display, also known as the hodograph plot, highlights the fact that errors at the tip of the cilium occur in correspondence to the largest positive values of the vertical velocity, *i.e.* in the acceleration phase from rest of the rigidly beating plate (see figure 5). In this type of plot we have represented the numerically obtained velocity data points with symbols, and the prescribed motion with a solid line.

Part of the discrepancies visible in figure 5 stems from the fact that to obtain the approximate value of the velocity for each point on the cilium, we have to perform a bilinear interpolation, after having identified the four nodes of the mesh which surround the chosen point on the cilium (since such a point would but very rarely coincide with a grid node).

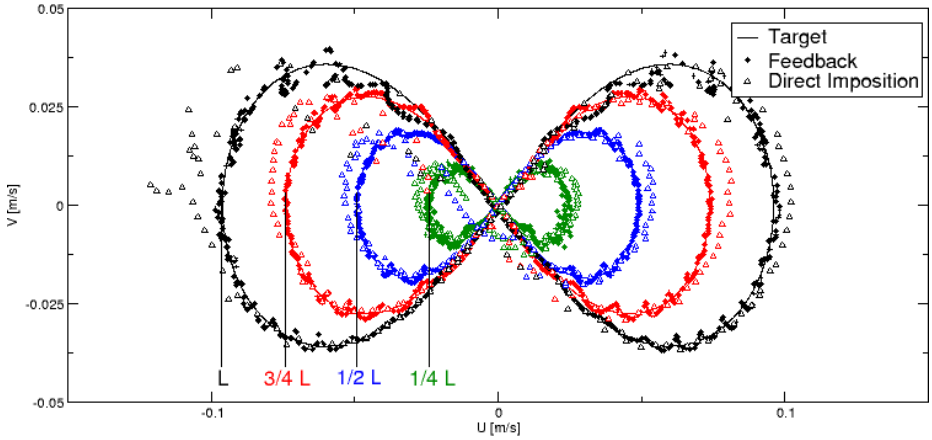


*Figure 5*. Velocity at different points within the rigidly beating cilium.

The feedback forcing coupled with the distribution approach used in NTMIX shows very precise results. On the other hand the direct forcing coupled with a linear interpolation in BRUTUS is more efficient, because the computational cost is over ten times lower.

Figure 6 illustrates the results obtained for the realistic beating of a single flexible cilium (second test case). Also here the best approach is found to be the combined use of the feedback forcing (with $\alpha_f = 0$) and the distribution strategy. One beating cycle is shown in figure 6; from the hodograph plane representation it appears that now the largest errors with respect to the target velocity occur halfway through the effective stroke phase of the cilium, when the vertical velocity attains its minimum value. In this case the maximum error in velocity amplitude occur again at the cilium tip and is equal to $20\%$ using the direct forcing and the linear interpolation technique.

In the initial transient, when the cilium starts oscillating in a fluid at rest, the behavior is as displayed in figure 2a where the velocity vectors are plotted together with color contours of the amplitude. During the effective stroke phase, when the cilium is almost straight, a high velocity region is created behind the cilium, near its tip. In the recovery phase, when a large part of the cilium moves quasi-tangentially to the wall, a vortex dipole is formed. In the subsequent cycle (not shown), this dipole is first sucked towards the wall and then ejected away from it. It is precisely this kind of behavior which lies at the heart of the propulsive efficiency of the *Pleurobrachia*.

Both methods have been used on all the cases to follow, leading to the same results. We consider this method an accurate procedure to analyze the flow field around bodies moving at relatively high frequencies within a fluid; we thus proceed with a parametric study of the motion of arrays

of cilia executing an antiplectic metachronal wave, with the goal of identifying efficient beating parameters.

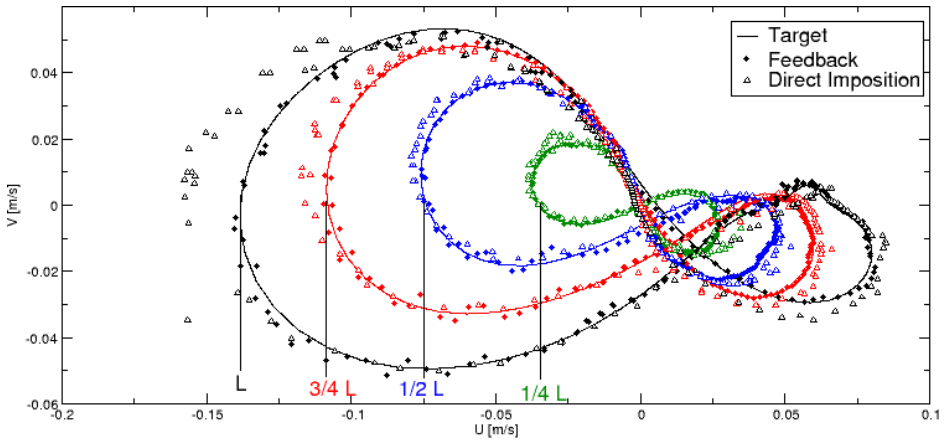


*Figure 6.* Velocity at different points within a realistically beating cilium.

## 3. Results

A snapshot of the velocity vectors is provided in figure 7a for the case of 9 cilia (comb plates) beating at 5Hz, together with colour surfaces of the amplitude of the velocity.

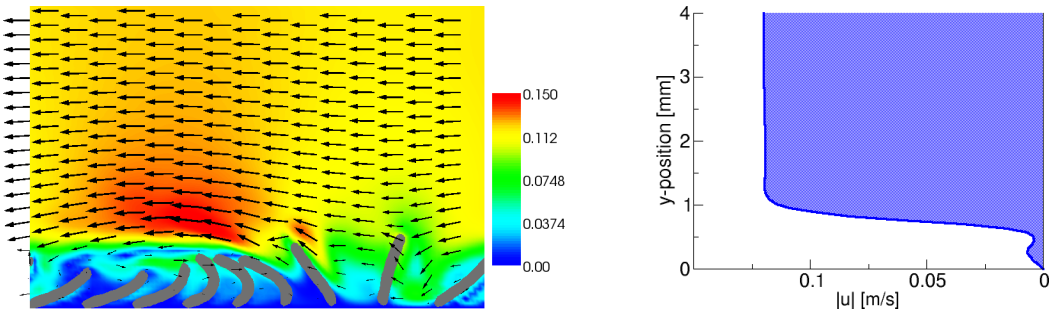


(a) Snapshots of velocity vectors. (b) Longitudinal velocity averaged in space and time.

*Figure 7.* $f = 5$Hz and $n = 9$ cilia.

The mean streamwise velocity profile is given in figure 7b. The wavelength $\lambda$ of the metachronal wave is always linked to the number of cilia $n$ present through the relation: $\lambda = nL/2$, *i.e.* the spacing between any two neighboring combs along the wall is fixed at $L/2$. The figure shows that in the sublayer region $(0 < y \leq L)$ the flow is sucked towards the wall during the effective stroke, when cilia are widely spaced apart, and ejected away from it during the recovery phase, when cilia are clustered near one another. The mean longitudinal velocity has a boundary layer-like profile lifted from the wall by $L/2$, in qualitative agreement with analytical results by Keller, Wu & Brennen [12].

The propulsive performances of the *Pleurobrachia* are related to the blowing/suction effect and are a direct function of the beating parameters. A study is thus called for to identify optimal parameters and to verify whether they match the swimming characteristics of the animal. The ability to associate the beating parameters to specific physical events is a prerequisite to the conception and realization of a technology capable of exploiting well-defined flow features and mimicking the motion of the *Pleurobrachia*.

Figures 8a and 8b show the $|u|$ and $v$ phase-averaged velocity profiles at $y = 0.9L$ as function of $\lambda x$ for the same case as above. The modulus of the longitudinal component of the velocity and the vertical component display simultaneously their maximum values approximately halfway through the wavelength, *i.e.* towards the end of the effective stroke phase, while $|u|$ attains its minimum value during the recovery phase. The $v$ component is equally distributed in $x$ about

positive and negative values (*cf.* figure 8b), mimicking blowing and suction through a fictitious wall; this indicates that the assumptions inherent to the analytical envelope model [10, 11] would be poorly satisfied in this case. Integrating along the longitudinal distance, an average $v$ close to zero is found, whereas an average velocity $u_{mean}$ equal to $-82$ mm/s at $y = 0.9L$ is obtained, reflecting the fact that the organism is propelled towards the right.

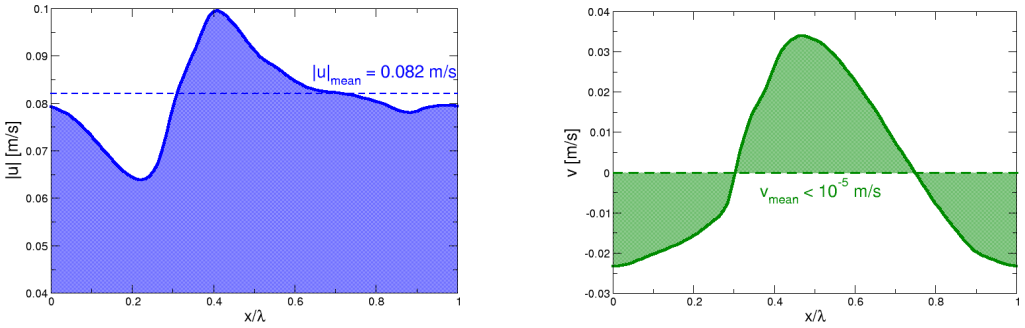


(a) Modulus of the longitudinal velocity $|u|$. (b) Vertical velocity $v$.

*Figure 8*. Phase-averaged velocity profiles at $y = 0.9L$.

It is simple to derive the energy equation, and to find the terms which contribute the most to an increase of the kinetic energy of the flow. By taking the integral over a volume $V$ (limited in $y$ between 0 and $L$ and running through a wavelength in $x$) of the scalar product of the Navier-Stokes equations with $\mathbf{u}$, it is easy to find:

$$\frac{d}{dt}\int_V (\frac{1}{2}\mathbf{u}.\mathbf{u})\, dV = P + D + S, \tag{5}$$

where $P$ is a production term, $D$ is a negative-definite dissipation term, and $S$ is a source term related to the presence of a volume force $\mathbf{f}$, with

$$P = \int_V (-u\, v)\, (u_y + v_x)\, dV, \tag{6}$$

$$D = -\nu \int_V \left[(u_x)^2 + (v_x)^2 + (u_y)^2 + (v_y)^2\right]\, dV, \tag{7}$$

$$S = \int_V \mathbf{u}.\mathbf{f}\, dV, \tag{8}$$

and subscripts denote partial derivatives. It is found that in all cases considered, the source term, linked to the beating power expended by the *Pleurobrachia* to move through water, is completely balanced by the action of viscosity.

**Parametric study and discussion**

Barlow & Sleigh [22] observed that the *Pleurobrachia* uses a combination of beating frequency and number of cilia per wave specific for each speed : 5 Hz and 25 cilia for low speed, 15 Hz and 12 cilia for average speed, 25 Hz and 9 cilia for escape/hunting speed (short bursts). To understand this natural optimization, the propulsive performances of ctenophores are studied, the frequency varying from 5 Hz to 25 Hz and the number of cilia varying from 9 to 25. In Table 1 the performances *per cilium* are reported and the sets of parameters used in nature are displayed in bold. The power output is defined by the energy transfer from the propulsive combplates to the flow, and the propulsive velocity $U$ by the longitudinal fluid speed observed when convergence is obtained. The latter is normalized by the maximal longitudinal velocity of the tip $U_{tip}$ and the results are displayed on the right side of Table 1.

The power output strongly increases with the frequency and decreases slowly with the number of cilia ($P \sim f^{2.5} n^{-0.3}$). It can be underlined that the natural power output varies much, over two decades. Also the velocity ratio increases with the frequency and decreases slowly with the

number of cilia ($U/U_{tip} \sim f^{1.13} n^{-0.25}$). This ratio is over one for high frequencies, which means that the fluid is blowed from the comb plates, instead of being paddled.

We emphasize the two-dimensional character of the results presented here. Indeed in the three-dimensional case the power output would be lower, and the blowing effect less present. As expected, large values of the power output are found in the case of long waves and high beating frequencies. Such conditions are however very demanding on the side of the animal. They could only be produced in very short bursts, if at all. The ratio of propulsion speed to power is not maximized by the effective beating parameters of the *Pleurobrachia*, indicating that such a simple functional is not sufficient to capture all the features involved in the propulsion of ctenophores.

| | Power output (nW/cilium) | | | $U/U_{tip}$ | | | |
|---|---|---|---|---|---|---|---|
| | $n=9$ | $n=12$ | $n=25$ | | $n=9$ | $n=12$ | $n=25$ |
| $f$=5 Hz | 5.77 | 5.09 | **4.12** | $f$=5Hz | 0.92 | 0.91 | **0.75** |
| $f$=15 Hz | 94.44 | **78.13** | 59.50 | $f$=15Hz | 1.08 | **1.02** | 0.93 |
| $f$=25 Hz | **445.56** | 367.24 | 238.87 | $f$=25Hz | **1.18** | 1.14 | 1.01 |

*Table 1.* Comparative influence of beating parameters, number of cilia $n$ and beating frequency $f$, on the performances (power output and the ratio $U/U_{tip}$).

These results are then compared to those obtained experimentally by Barlow & Sleigh [22], although the latter authors approximate the power output in a very crude manner. The observed trend on power is in qualitative agreement, despite the fact that row data differ by up to one decade (*cf.* figure 9a) for high frequencies. Simulations show a fair agreement with experiment (*cf.* figure 9b) for the ratio $U/U_{tip}$ at low and average frequencies. The overestimation of the power output and propulsion velocity are mainly due to the type of simulations carried out. Indeed a more realistic three-dimensional simulation would allow fluid to escape from the sides, whereas in our case the fluid can only be ejected via the top surface. This leads to an overestimation of the blowing effect associated to propulsion which partially accounts for the difference between theory and measurements.

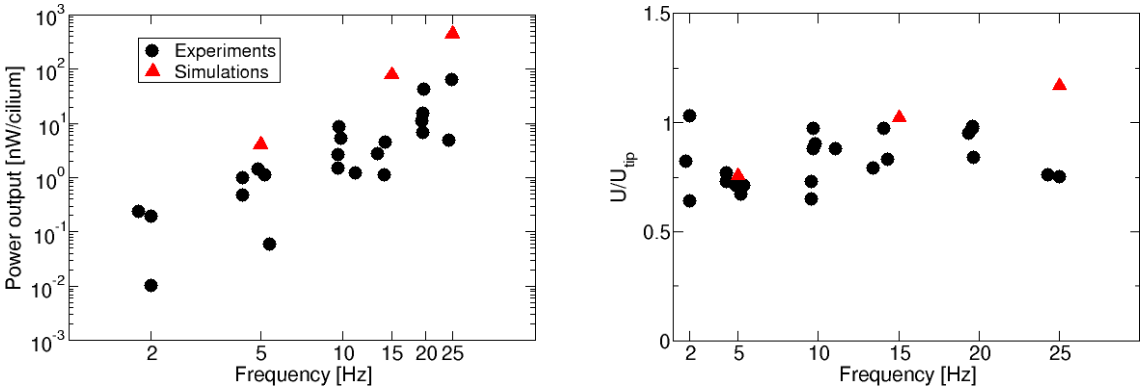


(a) Power outputs *per cilium*. (b) Propulsion speed $U$.

*Figure 9.* Comparison of power outputs and propulsion speed as function of the beating frequency.

## 4. Concluding remarks

The numerical procedure developed here using a coupling software (PALM) and an appropriate immersed boundary procedure is efficient and capable to model the influence of a flexible beating structure on the near-wall surrounding fluid. The specific application considered here focusses on the propulsive characteristics of a small ctenophore: it is shown that long waves oscillations with at high frequencies could yield very large propulsion velocity (a mechanism possibly exploited by the *Pleurobrachia* when in need of short bursts), and that the power output per cilium increases with frequency as $f^{2.5}$ during swim at natural conditions, in rough agreement with laboratory data. Also, it is noted that during its normal swimming phases, the animal does not simply

maximize the ratio of longitudinal propulsion velocity to power expended. Perspectives concern three-dimensional simulations and the complete interaction between freely beating comb plates and the fluid.

## References


[1] H. Lodish, A. Berk, L.S. Zipursky, P. Matsudaira, D. Baltimore, and J. Darnell. *Molecular Cell Biology*. Fourth Edition. W.H. Freeman and Co., New York, NY, 2000.

[2] L.J. Fauci and R.H. Dillon. Biofluidmechanics of reproduction. *Ann. Rev. Fluid. Mech.*, 38:371–394, 2006.

[3] A. Schweickert, T. Weber, T. Beyer, P. Vick, S. Bogusch, K. Feistel, and M. Blum. Cilia-driven leftward flow determines laterality in *Xenopus* . *Current Biology*, 17:60–66, 2007.

[4] M.B. Gardiner. The importance of being cilia. *Howard Hughes Medical Institute Bulletin*, 18(64):33–36, 2005.

[5] G. I. Taylor. Analysis of the swimming of microscopic organisms. *Proc. Royal Soc.*, A209:447–461, 1951.

[6] C. Brennen and H. Winet. Fluid mechanics of propulsion by cilia and flagella. *Ann. Rev. Fluid. Mech.*, 9:339–398, 1977.

[7] A.J. Reynolds. The swimming of minute organisms. *J. Fluid Mech.*, 23:241–260, 1965.

[8] E.O. Tuck. A note on a swimming problem. *J. Fluid Mech.*, 31:305–308, 1968.

[9] J.R. Blake. A spherical envelope approach to ciliary propulsion. *J. Fluid Mech.*, 46:199–208, 1971.

[10] J.R. Blake. Infinite models for ciliary propulsion. *J. Fluid Mech.*, 49:209–222, 1971.

[11] C. Brennen. An oscillating-boundary-layer theory for ciliary propulsion. *J. Fluid Mech.*, 65:799–824, 1974.

[12] S.R. Keller, T.Y. Wu, and C. Brennen. A traction layer model for ciliary propulsion. In *Plenum Press, New York*, pages 253–271, Pasadena, Ca., July 8-12 1974 1975.

[13] J.L. Lighthill. Flagellar hydrodynamics. *SIAM Rev.*, 18:161–230, 1976.

[14] N. Phan-Thien, T. Tran-Cong, and M. Ramia. A boundary element analysis of flagellar propulsion. *J. Fluid Mech.*, 184:533–549, 1987.

[15] G.I. Matsumoto. Swimming movements of Ctenophores, and the mechanics of propulsion by ctene rows. *Hydrobiologia*, 216-217:319–325, 1991.

[16] D. Barlow, M.A. Sleigh, and R.J. White. Water flows around the comb plates of the Ctenophore *Pleurobrachia* plotted by computer: a model system for studying propulsion by antiplectic metachronism. *J. Exp. Biol.*, 177:113–128, 1993.

[17] R. Mittal and G. Iaccarino. Immersed boundary methods. *Ann. Rev. Fluid. Mech.*, 37:239–261, 2005.

[18] B. Cuenot, B. Bédat, and A. Corjon. NTMIX3D - User's guide. Technical report, CERFACS, 1997.

[19] S. Buis, A. Piacentini, and D. Déclat. PALM: a computational framework for assembling high-performance computing applications. *Concurrency and Computation: Practice and Experience*, 18(2):231–245, 2005.

[20] E. A. Fadlun, R. Verzicco, Orlandi P., and J. Mohd-Yusof. Combined immersed-boundary finite difference methods for three-dimensional complex flow simulations. *J. Comp. Phys.*, 161:35–60, 2000.

[21] C. S. Peskin. The immersed boundary method. *Acta Numerica*, 11:479–517, 2002.

[22] D. Barlow and M.A. Sleigh. Water propulsion speeds and power output by comb plates of the Ctenophore *Pleurobrachia pileus* under different conditions. *J. Exp. Biol.*, 183:149–163, 1993.